When does vapor pressure deficit drive or reduce evapotranspiration?

A. Massmann[1], P. Gentine[1], C. Lin[2]

[1]Department of Earth and Environmental Engineering, Columbia University, New York, NY 10027
[2]Department of Hydraulic Engineering, Tsinghua University, Beijing, CN

Key Points:

- = enter point 1 here =
- = enter point 2 here =
- = enter point 3 here =

Corresponding author: Adam Massmann, `akm2203@columbia.edu`

Abstract

= enter abstract here =

1 Introduction

Changes to vapor pressure deficit (VPD) alter the atmospheric demand for water from the land surface. However, plant stomata have evolved to optimally regulate the exchange of water and carbon between vegetation and the atmosphere [**?**]. Therfore, an increase (decrease) in VPD may not correspond to an increase (decrease) in evapotranspiration (ET) because stomatal closure (opening) can cancel the effects of shifts to atmospheric demand.

Quantifying the plant response to a perturbation to atmospheric VPD increases our understanidng of feedbacks between the land surface and the atmosphere. If plant reponse reduces ET in response to an increase in VPD, the land surface will contribute a positive feedback in reponse to atmospheric drying. Conversely, if plant response increases ET in response to increase in VPD, then the land surface will contribute a negative feedback to atmospheric drying. The sign of these feedbacks drives the evolution of the atmosphere and landsurface at many timescales, from diurnal to interdecadal.

Here we use a Penman-Monteith framework to quantify plant reponse to perturbations to atmospheric demand for water. Section 2 derives the framework, Section 3 describes the data used, Section 4 presents results, and Section 5 discusses conclusions. The goal of this paper is to use reasonable approximations as a tool to increase intuition for plant response to atmospheric drying. This intuition will aid interpretation of observations and full complexity climate models.

2 Methods

The Penman-Monteith equation (hereafter PM) estimates ET as a function of atmospheric and land-surface variaibles:

$$ET = \frac{\Delta R + g_a \rho_a c_p D_s}{\Delta + \gamma(1 + \frac{g_a}{g_s})}, \tag{1}$$

where variable definitions are given in Table 1. **?** developed a model for g_s by combining optimal photosynthesis theory with empiracle approaches. The result for leaf-scale stomatal resistance was:

$$g_{l-s} = g_0 + 1.6\left(1 + \frac{g_1}{\sqrt{D_s}}\right)\frac{A}{c_s} \tag{2}$$

This can be adapted to an ecosystem-scale stomatal resistance by multiplying by leaf area index (LAI) and converting units to m s^{-1}:

$$g_s = \text{LAI}\,\frac{R*T}{P}\left(g_0 + 1.6\left(1 + \frac{g_1}{\sqrt{D_s}}\right)\frac{A}{c_s}\right) \tag{3}$$

While Equation 3 can be used in PM, it will make analytical work with the function intractable because A is a relatively strong function of ET. To remove dependence of ET on A we can use the semi-impiracle results of **?**. **?** showed that:

$$uWUE = \frac{GPP \cdot \sqrt{D}}{ET} \tag{4}$$

Table 1. Definition of symbols and variables

Variable	Description	Units
e_s	saturation vapor pressure	Pa
T	temperature	K
Δ	$\frac{\partial e_s}{\partial T}$	Pa K^{-1}
R	net radiation at land surface minus ground heat flux	W m^{-2}
g_a	atmospheric conductance	m s^{-1}
ρ_a	air density	kg m^{-3}
c_p	specific heat capacity of air at constant pressure	J K^{-1} kg^{-1}
D	VPD	Pa
γ	psychrometric constant	Pa K^{-1}
g_s	stomatal conductance	m s^{-1}
g_{l-s}	leaf-scale stomatal conductance	mol m^{-2} s^{-1}
$R*$	universal gas constant	J mol^{-1} K^{-1}
LAI	leaf area index	-
c_s	CO_2 concentration	μ mol CO_2 mol^{-1} air

^{a}Footnote text here.

is relatively constant across time and space (within plant functional type). If, following **?**, we approximate g_0 as 0, we can use uWUE to remove A from g_s in a way that makes PM analytically tractable:

$$g_s = \text{LAI} \frac{R * T}{P} 1.6 \left(1 + \frac{g_1}{\sqrt{D_s}}\right) \frac{uWUE \ ET}{c_s \ \sqrt{D}} \tag{5}$$

Plugging Equation 5 into Equation 1 and rearranging gives:

$$ET = \frac{\Delta R + \frac{g_a P}{T} \left(\frac{c_p D_s}{R_{air}} - \frac{\gamma c_s \sqrt{D}}{\text{LAI} \ R* \ 1.6 \ \text{uWUE} \left(1 + \frac{g_1}{\sqrt{D}}\right)}\right)}{\Delta + \gamma} \tag{6}$$

We can then take the derivative with respect to D to determine ecosystem reponse to atmospheric demand perturbations:

$$\frac{\partial \ ET}{\partial \ D} = \frac{g_a P}{T(\Delta + \gamma)} \left(\frac{c_p}{R_{air}} - \frac{\gamma c_s}{\text{LAI} \ 1.6 \ R \ \text{uWUE}} \left(\frac{2 g_1 + \sqrt{D}}{2 (g_1 + \sqrt{D})^2}\right)\right) \tag{7}$$

Note that given yearly uWUE from **?**, g_1 from **?** [as presented in **?**], and observations of R, T, P, D_s, and wind speed (WS), the only unknown is LAI. With flux tower observations of ET, LAI will then be uniquely determined for each observation through Equation 6:

$$LAI = -\frac{g_a \gamma c_s \sqrt{D_s} P}{\left(\text{ET} \ (\Delta + \gamma) - \Delta R - g_a \rho_a c_p D_s\right) 1.6 \ R \ T \ \text{uWUE} \left(1 + \frac{g_1}{\sqrt{D_s}}\right)} \tag{8}$$

This "pseudo-LAI" is some part "true" LAI (a measure of leaf area), and some part model and observational error, including error involving our assumption of constant uWUE. By calculating a unique LAI for each observation we will progate any model and observational uncertainty forward into our expression for $\frac{\partial \ ET}{\partial D}$.

Table 2. Plant functional types, their abbreviation, Medlyn coefficient [from **?**], and uWfUE [from **?**]. Note that units are converted such that the quantities fit into Equations 1-8 with the variables in Table 1.

Abbreviation	PFT	g_1 (Pa$^{0.5}$)	uWUE (μ-mol [C] Pa$^{0.5}$ J^{-1} [ET])
CRO	cropland	183.1	3.80
CSH	closed shrub	148.6	2.18
DBF	deciduous broadleaf forest	140.7	3.12
ENF	evergreen needleleaf forest	74.3	3.30
GRA	grassland (C3)	166.0	2.68

^{a}Footnote text here.

3 Data

We use data from FLUXNET2015. Because g_1 coefficients [**?**] and uWUE were only both available for five plant functional types (PFTs - see Table 2), only 56 of the 77 sites were used. Figure 1 presents each site and its plant functional type.

p

We restrict our analysis to the daytime (sensible heat > 5 W m^{-1} and shortwave radiation > 50 W m^{-2}) when there is no precipitation and the plants are growing (GPP > 10% of the 95th pecentile). Also, because some sites use half hourly data but some use hourly, we aggregate all data to hourly averages. Only times with good quality control flags are used.

4 Results

By construction, the variability in the LAI term (Equation 8) contains all model and observational uncertities. LAI also has physical meaning corresponding to "true" leaf area, and we expect that it would be approximately $O(1)$. We can have some confidence in our framework, including the assumption of constant uWUE, if calculated LAIs are generally $O(1)$. Figure 2 presents the histogram of calculated LAIs with outliers (lowest and highest 5% percent) and unphysical values (LAI < 0.) removed. All remaining LAI values are $O(1)$ which provides confidence in model framework.

An additional concern is that the LAI term may in fact be some function of D, in which case the dependence would need to be accounted for when taking the derivative. Figure 3 plots the joint distrivution of LAI and VPD, and shows that LAI is very weakly a function of VPD. Given this weak dependence, we argue that Equation 7 is a valid approxiamtion for ET response to D.

Before diving into calculated values of $\frac{\partial ET}{\partial D}$, it is useful to consider the functional form of Equation 7. There are three terms: a scaling term for the full expression we will call Term 1 ($\frac{g_a P}{T(\Delta+\gamma)}$), a relatively constant offset we will call Term 2 ($\frac{c_p}{R_{air}}$), and a variable term we will call Term 3 ($\frac{\gamma c_s}{\text{LAI} 1.6 R \text{ uWUE}} \left(\frac{2g_1+\sqrt{D}}{2(g_1+\sqrt{D})^2} \right)$). All variables are positive, so the relative magnitude between Term 2 and Term 3 will determine the sign of the derivative, while Term 1 will scale the expression larger or smaller.

In Term 1, $\frac{P}{T} \propto \rho$, so this should vary little relative to g_a and Δ. γ should also be relatively constant, So the scaling term, Term 1, should be primarily a function of g_a and temperature (through the function Δ). While temperature range may vary for PFT, the fucntional form of Δ will be the same. g_a will vary strongly with PFT due to the importance of surface roughness. However, the coeffiecent of variability for g_a is relatively constant across PFT.

So, the influence of g_a on the relative (to the mean) variability of Term 1 is approximately similiar across PFT.

Figure 4A shows Term 1 normalized by mean g_a (calcualted for each plant functional type), and confirms that much of the relative variability of Term 1 is contained in the g_a term's relative variability. Additionally, the impact of T on the relative variability increases with increasing g_a.

While the relative variability of Term 1 is similiar across PFT, the absolute value of Term 1 varies strongly across PFT. Figure 4B shows Term 1 evaluated with the mean g_a for each PFT, and at the range of observed temperatures for each PFT. As expected, for the tree PFTs (DBF, ENF) Term 1 is much larger and the temperature dependence is much stronger. Systematic differences in observed temperatures also cause differences in the average magnitude of Term 1. For example, ENF experiences on average colder temperatures and is thus more likely to have a larger scaling term. Additionally, because $std(g_a) \propto \overline{g_a}$, the spread of Term 1 due to g_a variability will be larger, although this is not shown for simplicity. To summarize, the variability of Term 1 will look like Figure 4A for each PFT, but the scale of the x and y-axis will increase or decrease according to Figure 4B.

"just say that vpd effect is approximately linear (except at low VPD), and then say so we are most concerned about when d et/dvpd is zero, as this is the minima. then you can just look at this treshold as a function of LAI, uWUE, and g1."

Term 2 minus Term 3 determines the sign and magnitude that the scaling Term 1 is multiplied by. If we assume that c_s variability is relatively less than LAI and D variability, then variability within PFT will be soley detmined by LAI and D. Figure 5 shows how (Term 2 - Term 3) varies with D and LAI, as a function of PFT. In Figure 5a lower uWUE and LAI shift the disrtribution of (Term 2 - Term 3) towards negative values. Additionally, the smaller $g1$, the greater the relative D dependence of of (Term 2 - Term 3). This is observed most strongly for the ENF PFT, which has the smallest $g1$ (74.31).

Figure 5b shows the location of the minima of ET, as a function of LAI and D. For any LAI or VPD less (more) than these curves, Term 2 - Term 3 will be negative (positive). It is clear that the portion of VPD observations below these curves will be a strong function of LAI. However, we can see some general trends. For CSH, $\frac{\partial ET}{\partial D}$ should be negative for the vast majority of observed LAI and VPD. The split appears to be more even among ENF, GRA, and DBF, and we might expect a greater frequency of positive $\frac{\partial ET}{\partial D}$ for CRO.

Table 3 confirms these expectations for PFT behaviour of $\frac{\partial ET}{\partial D}$. For all PFTs except for CRO, average $\frac{\partial ET}{\partial D}$ is less than zero. However, $\frac{\partial ET}{\partial D}$ evaluated at the average of all variables (e.g. LAI, T, c_s, D) is only negative for CSH and GRA. And, DBF in addition to CRO experiences $\frac{\partial ET}{\partial D} < 0$ less than half the time. These observations highlight the effect of the nonlinear function in Figure 5: $\frac{\partial ET}{\partial D}$ has a much steeper slope when the function is negative, and is thus more likely to be large magnitude.

The units of $\frac{\partial ET}{\partial D}$ make it difficult to interpret if D is even a meaningful contributor to ET's variability. To understand D's contribution better, we use a linear approximation and present $\frac{\partial ET}{\partial D}$ multiplied by D's standard deviation. The range of D's contribution to ET's variability ranges between 16 - 20 W m^{-2} for all PFTs except for CSH, which is about 51 W m^{-2}. Another meaningful comparison is to $\frac{\partial ET}{\partial R} * std(R)$, as net radiation generally the driver of ET (cite joe berry here). For all PFTs except for CSH D contributes between 14.5 - 20.5 % of R's contribution to variability. For CSH the portion is much larger, about 44 %. However it is important to note that a linear approximation about a mean base state is probably not a very good approximation across the range of variabilility, so these values are just estimates of D's contribution to ET's variability.

So far, idealized plots and statistics have illuminated the form of $\frac{\partial ET}{\partial D}$ and how it varies with PFT. Large mean LAI and uWUE shifts CRO and DBF towards positive $\frac{\partial ET}{\partial D}$. How-

Table 3. Statistics of $\frac{\partial ET}{\partial D}$ as a function of PFT.

PFT	$\overline{\frac{\partial ET}{\partial VPD}}$	$\frac{\partial ET}{\partial D}\left(\overline{T,\ldots,D}\right)$	$\frac{\partial ET}{\partial D}\left(\overline{T,\ldots,D}\right)*\text{std}(D)$	$\frac{\frac{\partial ET}{\partial D}(\overline{T,\ldots,D})*\text{std}(D)}{\frac{\partial ET}{\partial R}(\overline{T,\ldots,D})*\text{std}(R)}$	fraction $\frac{\partial ET}{\partial VPD}<0.$
CRO	0.000853	0.026241	18.523659	0.203022	0.473311
CSH	-0.108234	-0.091526	50.861613	0.439379	0.931660
DBF	-0.012727	0.013794	19.734435	0.164241	0.461674
ENF	-0.034087	0.000706	16.611852	0.148548	0.534425
GRA	-0.019637	-0.000921	16.798083	0.173552	0.631735

[a]Footnote text here.

ever, the strongly nonlinear funtion of $\frac{\partial ET}{\partial D}$ at $\frac{\partial ET}{\partial D}<0$ pushes $\overline{\frac{\partial ET}{\partial D}}$ negative for DBF (it does not do this for CRO because of CRO's high $g1$). ENF's low $g1$ value increases the dependence of $\frac{\partial ET}{\partial D}$ on D, and makes the function more strongly nonlinear. This has the side effect of pushing $\overline{\frac{\partial ET}{\partial D}}$ negative futher than other PFTs for a given fraction $\frac{\partial ET}{\partial D}<0$ and magntiude $\frac{\partial ET}{\partial D}(\overline{T,\ldots,D})$. GRA shows the opposite behavior; a relatively high $g1$ makes the function more linear, decreasing the magnitude of $\overline{\frac{\partial ET}{\partial D}}$ for a given fraction $\frac{\partial ET}{\partial D}<0$ and magntiude $\frac{\partial ET}{\partial D}(\overline{T,\ldots,D})$ (although g_a and Term 1 also probably have a role in this). Finally, low $uWUE$ of CSH pushes to toward by far the lowest values $\frac{\partial ET}{\partial D}$ (Figure 5). Variability in D accounts for the largest about of ET variability for CSH. For the other PFTs, D contributes less to ET variaibiliyt, but still represents about 15-20 % of R's contributions to ET variability.

4.1 Full observations of $\frac{\partial ET}{\partial D}$

Now that we have an intuitive understanding of $\frac{\partial ET}{\partial D}$'s behavior, we are equipped to intepret fully realistic plots of $\frac{\partial ET}{\partial D}$ for each PFT. Figure **??** presents calculated $\frac{\partial ET}{\partial D}$ where, unless otherwise noted, all variables in Equation 7 are allowed to vary.
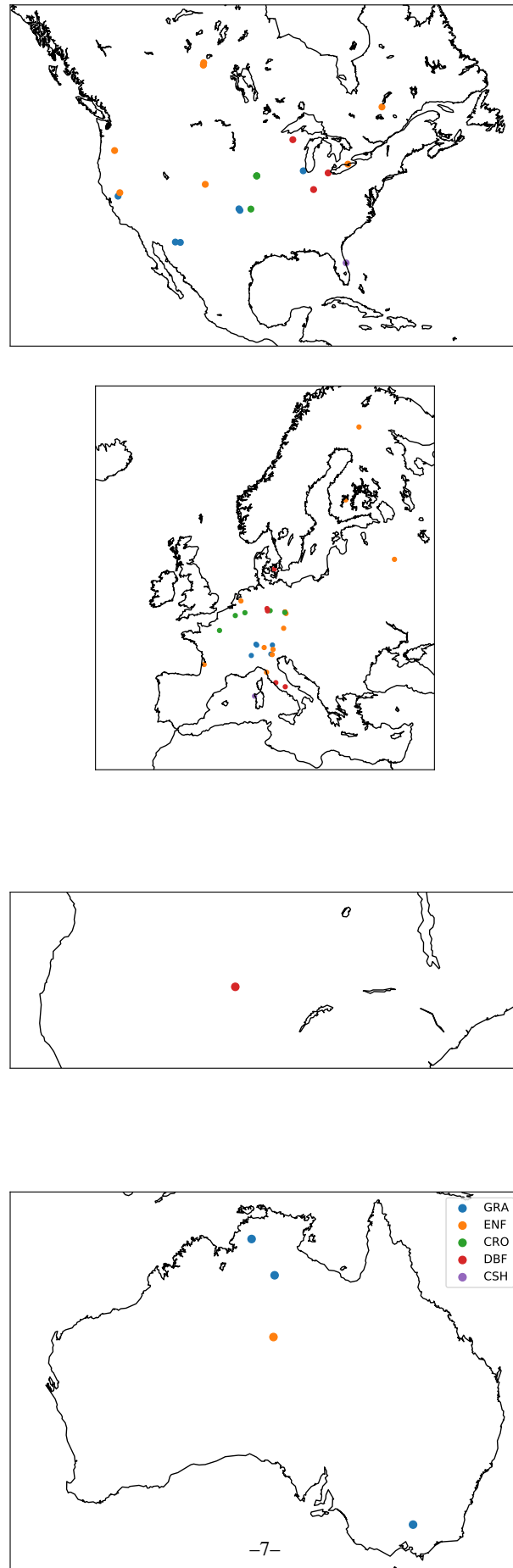
$$\tag{9}$$

Figure 1. Plant functional type and location of sites used in analysis. Note should probably just split this into 4 continents (US, Europe, Africa, Australia).
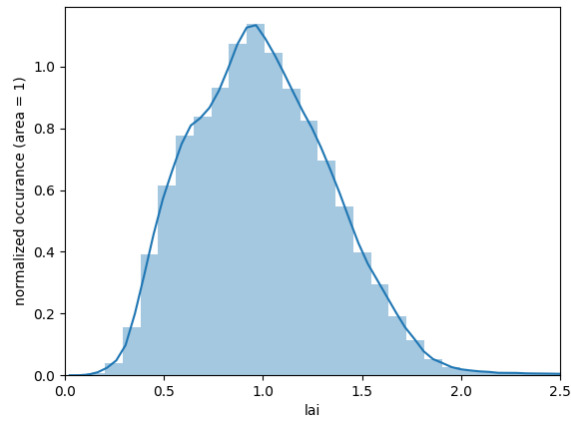
Figure 2. Histogram of LAI values calculated for each site and time according to Equation 8. The lowest and highest 5% are removed as outliers, as well as any values below 0. The curve is normalized such that its area is 1.
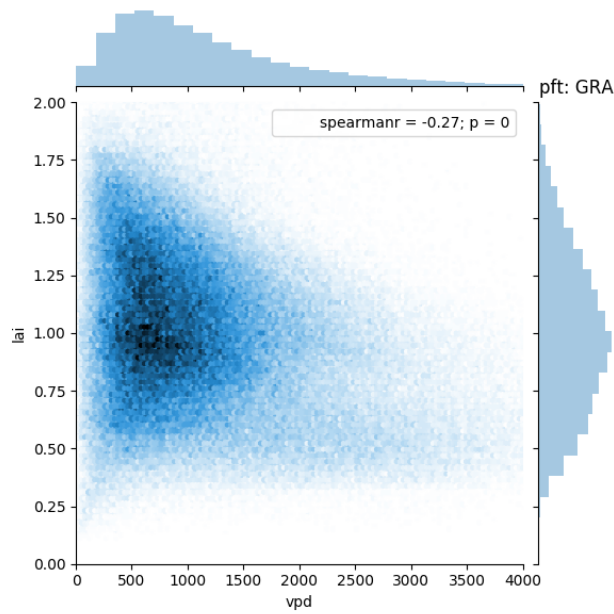

Figure 3. The joint distribution of D and LAI. LAI has only a weak dependence on D
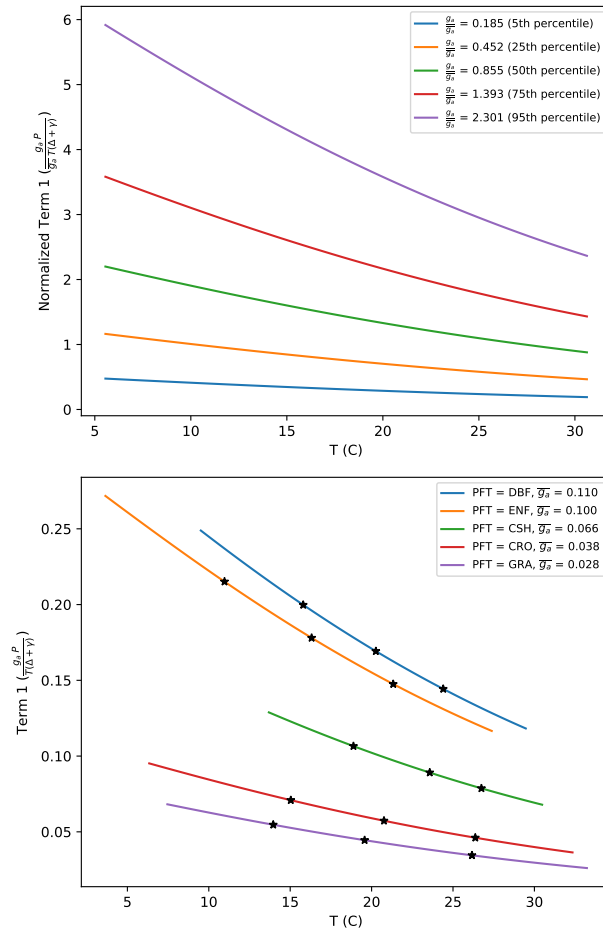
Figure 4. Primary sources of variability for Term 1. A) Variability within each PFT: Term 1 normalized by mean g_a for each PFT. B) Variability between each PFT: Term 1 evaluated at mean g_a for each PFT. Temperature range is 5-95th percentile for each PFT. Additionally, stars denote the location of the 25th, 50th, and 75th percentiles.
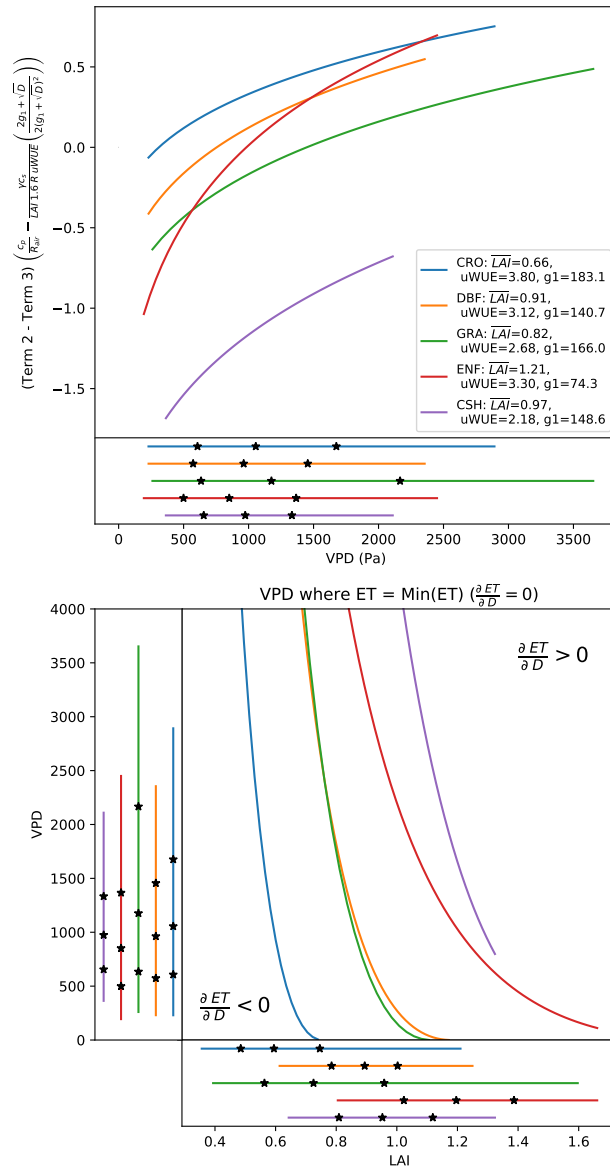
Figure 5.

135